JOURNAL OF COMPUTATIONAL PHYSICS 63, 458–476 (1986)

Discrete Models for the Numerical Analysis of Time-Dependent Multidimensional Gas Dynamics*

PHILIP L. ROE

College of Aeronautics, Cranfield Institute of Technology, Cranfield MK43 0AL, United Kingdom

Received February 7, 1985; revised May 31, 1985

This paper explores a possible technique for extending to multidimensional flows some of the upwind-differencing methods that have proved highly successful in the one-dimensional case. Attention here is concentrated on the two-dimensional case, and the flow domain is supposed to be divided into polygonal computational elements. Inside each element the flow is represented by a local superposition of elementary solutions consisting of plane waves not necessarily aligned with the element boundaries.

1. INTRODUCTION

The recent survey of Woodward and Colella [16] shows that for one-dimensional gas dynamics there is an order of magnitude difference in effectiveness between sophisticated codes physically based on correct transfer of information, and simpler codes combining central differences with artificial viscosity. The sophisticated codes need much more computational work to update the solution at each mesh point, but this is far outweighed by their ability to capture discontinuities on a coarser mesh. For two-dimensional problems the difference in efficiency is far less marked, and for less violent flows than the ones they consider the advantage is likely to be reversed.

The explanation is probably that the physics of one-dimensional flow is especially simple and well understood, and easy to imitate by numerical processes. Two-dimensional flows are more complex; in particular, acoustic waves can propagate in infinitely many directions rather than just two, and vorticity exists as a new phenomenon. Most extensions of upwind codes to two or more dimensions ignore these issues and advance the solution by "splitting," that is to say, through a sequence of one-dimensional operators. For examples, see the survey by Woodward and Colella, also Sells [13] and Chakravarthy and Osher [1]. There are also what may be called "one-and-a-half-dimensional" methods, in which the one-dimensional operators are interwoven, but the underlying physical model is still one involving

* Research was supported in part by the National Aeronautics and Space Administration under Contract NAS1-17070 while the author was in residence at the Institute for Computer Applications in Science and Engineering, NASA Langley Research Center, Hampton, Va. 23665.

0021-9991/86 $3.00

wave propagation along the coordinate directions. This approach seems to yield some modest gains, as shown by Lytton [7] and Colella [2]. However, an observation is made in Section 3 which casts doubt on its real value.

If full advantage can be taken of upwinding techniques in two or more dimensions it is probably necessary to devise methods which take account of the actual directions in which information is propagated. The only results so far available for a method of this kind are those of Davis [4]. He assumes that the flow is locally dominated by a single shock wave whose unknown orientation may be deduced from the velocity field, or, in a later version of the code, from the pressure field (Davis, private communication). His method works very well on test problems where the flow is divided by shock waves into piecewise uniform regions. This is encouraging because it shows that a well chosen model of the flow can be used to numerical advantage.

It has been conjectured that the way forward into two dimensions is blocked by the complexity of a "two-dimensional Riemann solver," by which is meant an algorithm for computing the breakdown of initial conditions which are piecewise constant in two-dimensional cells. The solution of this problem close to the edge of a cell is straightforward, but secondary interactions near the corners are extremely difficult to compute. Even if a Riemann solver of this kind were computationally feasible, however, it would not be a satisfactory building block for two-dimensional calculations. It would, like the operator-splitting methods mentioned above, force the principal wave motions to take place normal to the cell boundaries.

In the present work we avoid this difficulty by thinking of the data as piecewise linear rather than piecewise constant, and in Section 2 we interpret one-dimensional upwinding schemes in that light. The gradients in the data are used to construct a "model flow" consisting of simple waves within each mesh interval. In Section 3 the corresponding simple wave solutions, propagating in arbitrary directions, are derived for the two-dimensional equations. In Section 4 we propose model flows which can be fitted to any data which varies linearly in two dimensions, and in Section 5 we describe a strategy for constructing conservative differencing schemes by fitting such models to the data given at vertices of an irregular two-dimensional mesh. Section 6 contains observations on the possibility of extending the work to three-dimensional flow, and Section 7 comments on the type of advection scheme needed to complete the algorithm.

2. Upwinding in One Dimension

We begin by observing that one way to derive upwind schemes for the Euler equations in one dimension is to suppose that the flow in each mesh interval $(i, i+1)$ is a locally linear superposition of simple waves having the form

$$\mathbf{w}(x, t) = \sum_k (\alpha_k \mathbf{r}_k) \cdot (x - \lambda_k t). \tag{2.1}$$

Here, $\mathbf{w}$ is the vector of unknowns, $\mathbf{r}_k$ is an eigenvector showing how the gradients due to the kth wave are distributed over the components of $\mathbf{w}$, α_k is the amplitude of the kth wave, and λ_k its speed. Any independent set of unknown variables $\mathbf{w}$ may be chosen, and the choice will not affect the values of α_k, λ_k, but $\mathbf{r}_k$ will be different for each choice. The values of $\lambda_{1,2,3}$ are

$$u-a,\ u,\ u+a \tag{2.2}$$

and the values of $\alpha_{1,2,3}$ are

$$\frac{1}{2a^2}[\Delta p-\rho a\Delta u],\ \Delta\rho-\frac{1}{a^2}\Delta p,\qquad \frac{1}{2a^2}[\Delta p+\rho a\Delta u] \tag{2.3}$$

where $\Delta(\cdot)=(\cdot)_{i+1}-(\cdot)_i$ and any local average values of ρ, a, u are valid. To achieve a conservative algorithm, two conditions are necessary. The eigenvectors $\mathbf{r}_k$ must show the effects of the waves upon the conserved variables $(\rho, \rho u, \rho e)$. In these variables $\mathbf{r}_1, \mathbf{r}_2, \mathbf{r}_3$ are given by

$$\mathbf{r}_1=\begin{vmatrix}1\\ u-a\\ h-ua\end{vmatrix},\qquad \mathbf{r}_2=\begin{vmatrix}1\\ u\\ \frac{1}{2}u^2\end{vmatrix},\qquad \mathbf{r}_3=\begin{vmatrix}1\\ u+a\\ h+ua\end{vmatrix}, \tag{2.4}$$

where $h=a^2/(\gamma-1)+\frac{1}{2}u^2$ is the specific enthalpy. Also, the average values of ρ, a, u must now be chosen so that

$$\sum \alpha_k\lambda_k\mathbf{r}_k=\Delta\mathbf{F}/\Delta x, \tag{2.5}$$

where $\mathbf{F}$ is the vector of flux quantities. For details, see [9, 12].

This may be throught of as constructing, within each interval $(i, i+1)$ a local model of the flow. The model consists of elementary solutions of the Euler equations, linearized about a particular local average state. The model matches the observed data with respect to the spatial derivatives (or to be precise, with respect to the mesh differences). The time evolution of the model flow is readily predicted, and provides the information which is used to advance the global solution through one time step.

For example, a first-order scheme to update the solution [12, 15] involves subtracting a quantity

$$\frac{\Delta t}{\Delta x}\alpha_k\lambda_k\mathbf{r}_k$$

from the value of $\mathbf{w}$ at whichever end of the interval the kth wave is moving towards, i.e., from $\mathbf{w}_i$ if λ_k is negative in $[i, i+1]$ or from $\mathbf{w}_{i+1}$ if λ_k is positive. This algorithm causes selected information to be transmitted in directions which are determined by the model flow.

The present paper is motivated by the wish to create algorithms having similar properties with regard to multidimensional wave propagation, but its content is limited almost entirely to the devising of appropriate multidimensional models. The author hopes to develop the corresponding time-marching algorithms in subsequent publications.

3. Elementary Solutions in Two Dimensions

In this section, as a necessary preliminary to the construction of two-dimensional models, we investigate the elementary solutions from which they may be built. Consider the Euler equations in primitive variables $\mathbf{w}_p = (p, u, v, \rho)$.

$$\begin{aligned} p_t + up_x + vp_y + \rho a^2(u_x + v_y) &= 0, \\ u_t + uu_x + vu_y + \frac{1}{\rho} p_x &= 0, \\ v_t + uv_x + vv_y + \frac{1}{\rho} p_y &= 0, \\ \rho_t + u\rho_x + v\rho_y + \rho(u_x + v_y) &= 0. \end{aligned} \tag{3.1}$$

Corresponding to Eq. (2.1) there are solutions to (3.1) of the form

$$\mathbf{w} = \alpha(\theta)\, \mathbf{r}(\theta)(x \cos\theta + y \sin\theta - \lambda(\theta)\, t), \tag{3.2}$$

where θ is an arbitrary angle, and $\mathbf{r}(\theta)$ is an eigenvector. For acoustic waves and primitive variables it can be shown that

$$\mathbf{r}(\theta) = \begin{vmatrix} \rho a^2 \\ a \cos\theta \\ a \sin\theta \\ \rho \end{vmatrix} \tag{3.3}$$

and that the wave speed is

$$\lambda(\theta) = u \cos\theta + v \sin\theta + a. \tag{3.4}$$

Figure 1 shows that this speed corresponds to a wave front tangential to the Mach cone. We repeat here an observation from Roe [10]. Consider two Cartesian points having the same value of y, in a flow given by (3.2)–(3.4). An operator-split

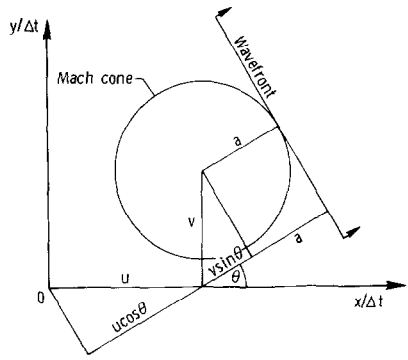

FIG. 1. An acoustic wave front.

method will attempt to explain the difference in states as due to waves passing in the x direction; it will compute

$$\Delta \begin{vmatrix} p \\ u \\ v \\ \rho \end{vmatrix} \propto \begin{vmatrix} \rho a^2 \\ a\cos\theta \\ a\sin\theta \\ \rho \end{vmatrix} = \tfrac{1}{2}(1+\cos\theta) \begin{vmatrix} \rho a^2 \\ a \\ 0 \\ \rho \end{vmatrix} + \sin\theta \begin{vmatrix} 0 \\ 0 \\ a \\ 0 \end{vmatrix} + \tfrac{1}{2}(1-\cos\theta) \begin{vmatrix} \rho a^2 \\ -a \\ 0 \\ \rho \end{vmatrix}, \tag{3.5}$$

where the r.h.s. shows the eigenvectors of two one-dimensional acoustic waves, and a slip line. These spurious waves may not even travel in the proper direction and their inclusion in a numerical method can hardly be realistic. This criticism applies even to the "unsplit" algorithms of Colella [2] and Lytton [7]. Our goal in the next section is to construct local models of the flow by superposing simple waves whose orientation is not assumed in advance.

Such a model cannot, however, be constructed purely out of acoustic waves since these are irrotational and the data may not be. There are two other fundamental flows which can be incorporated neatly into the model. One is a shear flow, which again has the general form of (3.2) but with

$$\mathbf{r}(\theta) = \begin{vmatrix} 0 \\ -\sin\theta \\ \cos\theta \\ 0 \end{vmatrix}, \tag{3.6}$$

$$\lambda(\theta) = u\cos\theta + v\sin\theta. \tag{3.7}$$

Another is solid-body rotation, or vorticity

$$u = -\tfrac{1}{2}\omega y, \qquad v = \tfrac{1}{2}\omega x. \tag{3.8}$$

There still remains an effect which is missing from the model, for all the flows above are isentropic. An entropy wave, across which pressure and velocity do not change, reveals itself in the primitive variables as a change of density. The general form is again (3.2) with $\lambda(\theta)$ given by (3.7), but with

$$\mathbf{r} = \begin{vmatrix} 0 \\ 0 \\ 0 \\ \rho \end{vmatrix} \tag{3.9}$$

independent of θ.

Another interesting fundamental solution (not directly used below) is obtained by superposing acoustic waves of the same strength with all possible propagation directions, i.e., by integrating (3.2) with respect to θ from 0 to 2π with $\alpha(\theta) = \alpha_0$. The result yields

$$\begin{aligned} p_x &= p_y = 0, \\ u_x &= v_y = \tfrac{1}{2}\alpha_0, \\ v_x &= u_y = 0, \\ \rho_x &= \rho_y = 0. \end{aligned} \tag{3.10}$$

This solution would appear in the data as a region of uniform (isotropic) velocity divergence. However, the same data could be explained equally well by the passage of four plane waves

$$\mathbf{w}(0) + \mathbf{w}(\pi/2) + \mathbf{w}(\pi) + \mathbf{w}(3\pi/2), \tag{3.11}$$

where $\mathbf{w}(\theta)$ is given by (3.2). For numerical purposes the discrete representation by four plane waves is more amenable than the representation by one circular wave, and this is how a uniformly diverging flow would be dealt with in the model we develop below. However, it may be worth noting that any three equal waves separated by angles of $2\pi/3$ would also produce (locally) the same effect.

4. The Discrete Models

It is not obvious how the model flows of Section 2 should be generalized from one dimension to two. The chief difficulty is that whereas in one dimension there are just three types of elementary wave, in two dimensions there are infinitely many if we count all the possible orientations as distinct. In one dimension there is only one model that can be constructed, and it has three parameters which are the unknown wave strengths. Matching the model to the spatial gradients of the three data quantities p, u, ρ gives three simple linear equations whose solution is (2.3). In two dimensions the data will allow us to estimate gradients in two directions of four

quantities, yielding eight items of information. Whatever model we choose must have eight free parameters, some of which may be wave amplitudes, and the remainder will be orientation angles. If all the orientations are supposed to be known (aligned, e.g., with the grid directions) we will again find easily solved linear equations for the amplitudes. However, because of the observation made concerning Eq. (3.5), we reject this approach, and require that at least some of the orientations be left unspecified. However, the equations which must be solved for the parameters then become nonlinear. If the free parameters are not judiciously chosen, no closed form solution may be possible, or the solution may not always be real-valued, or the solution may be computationally expensive. In such cases, the model will be useless.

Two models, however, have been found whose parameters are given by simple real-valued expressions for all data. Each has, as its representation of the acoustic disturbances, a set of four orthogonal waves (Fig. 2). One of the four will have an orientation angle in the range $[\pm\pi/4]$ and we take this as reference. Its orientation is θ, and its amplitude α_1. The strength of the wave which moves in the opposite direction will be α_2, and the waves which travel at right angles to these two have strengths α_3, α_4. To this model we add an entropy wave with strength β and inclination ϕ, so that the model now contains seven unknown parameters.

To close the model we must introduce a fundamental solution incorporating vorticity, and it is only in this respect that the two models differ. In Model A we introduce a uniform vorticity ω, and in Model B we introduce a shear flow such that

$$\begin{aligned} u &= u_0(1 + k(v_0 x - u_0 y)), \\ v &= v_0(1 + k(v_0 x - u_0 y)). \end{aligned} \tag{4.1}$$

This is a special case of (3.6), (3.7) with $\tan\theta = -(u/v)$. We will first show the algebra for Model A, which is slightly simpler.

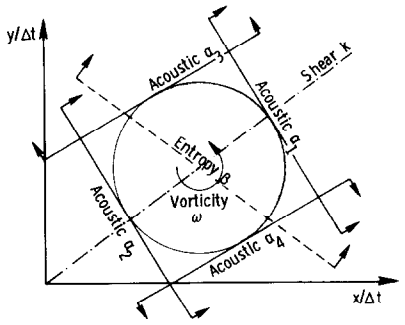

FIG. 2. The waves comprising the discrete models.

To tidy up the equations we write dimensionless derivatives

$$\begin{aligned} P_x &= p_x/\rho a^2, & P_y &= p_y/\rho a^2, \\ U_x &= u_x/a, & U_y &= u_y/a, \\ V_x &= v_x/a, & V_y &= v_y/a, \\ R_x &= \rho_x/\rho, & R_y &= \rho_y/\rho. \end{aligned} \tag{4.2}$$

By equating these to the sum of contributions produced by each component of the model, we find

$$P_x = \alpha_1 \cos\theta + \alpha_2 \cos\theta - \alpha_3 \sin\theta - \alpha_4 \sin\theta, \tag{4.3a}$$

$$P_y = \alpha_1 \sin\theta + \alpha_2 \sin\theta + \alpha_3 \cos\theta + \alpha_4 \cos\theta, \tag{4.3b}$$

$$U_x = \alpha_1 \cos^2\theta - \alpha_2 \cos^2\theta + \alpha_3 \sin^2\theta - \alpha_4 \sin^2\theta, \tag{4.3c}$$

$$U_y = \alpha_1 \sin\theta \cos\theta - \alpha_2 \sin\theta \cos\theta - \alpha_3 \sin\theta \cos\theta + \alpha_4 \sin\theta \cos\theta - \tfrac{1}{2}\omega/a, \tag{4.3d}$$

$$V_x = \alpha_1 \sin\theta \cos\theta - \alpha_2 \sin\theta \cos\theta - \alpha_3 \sin\theta \cos\theta + \alpha_4 \sin\theta \cos\theta + \tfrac{1}{2}\omega/a \tag{4.3e}$$

$$V_y = \alpha_1 \sin^2\theta - \alpha_2 \sin^2\theta + \alpha_3 \cos^2\theta - \alpha_4 \cos^2\theta, \tag{4.3f}$$

$$R_x = \alpha_1 \cos\theta + \alpha_2 \cos\theta - \alpha_3 \sin\theta - \alpha_4 \sin\theta + \beta \cos\phi, \tag{4.3g}$$

$$R_y = \alpha_1 \sin\theta + \alpha_2 \sin\theta + \alpha_3 \cos\theta + \alpha_4 \cos\theta + \beta \sin\phi. \tag{4.3h}$$

In these equations, the convention which distinguishes the contributions of α_1, α_2 is that the same angle θ is used, but the sign of a is reversed. The eight equations can be solved quite easily. From (4.3d) and (4.3e) we obtain at once

$$\begin{aligned} \omega &= a(V_x - U_y) \\ &= (v_x - u_y). \end{aligned} \tag{4.4}$$

Also

$$\begin{aligned} R_x - P_x &= \beta \cos\phi, \\ R_y - P_y &= \beta \sin\phi, \end{aligned} \tag{4.5}$$

whence β, ϕ. Next add (4.3d) and (4.3e) to obtain

$$U_y + V_x = 2 \sin\theta \cos\theta(\alpha_1 - \alpha_2 - \alpha_3 + \alpha_4) \tag{4.6}$$

and subtract (4.3f) from (4.3c)

$$U_x - V_y = (\cos^2\theta - \sin^2\theta)(\alpha_1 - \alpha_2 - \alpha_3 + \alpha_4). \tag{4.7}$$

Dividing (4.6) by (4.7) yields

$$\tan 2\theta = \frac{U_y + U_x}{U_x - V_y} = \frac{N}{D}. \tag{4.8}$$

Since we have defined $|\theta| \leqslant \pi/4$ this result defines a unique orientation which is always real, coinciding, in fact, with the principal axis of the strain tensor. With θ known, the remaining equations are linear. We write (4.3c) and (4.3f) as

$$U_x = (\alpha_1 - \alpha_2)\cos^2\theta + (\alpha_3 - \alpha_4)\sin^2\theta,$$
$$V_y = (\alpha_1 - \alpha_2)\sin^2\theta + (\alpha_3 - \alpha_4)\cos^2\theta,$$

and combine them to give

$$\alpha_1 - \alpha_2 = \frac{U_x \cos^2\theta - V_y \sin^2\theta}{\cos^2\theta - \sin^2\theta}. \tag{4.9}$$

This expression must be rewritten to avoid the possible singularity. Noting that

$$\cos^2\theta = \tfrac{1}{2}(1 + \cos 2\theta), \qquad \sin^2\theta = \tfrac{1}{2}(1 - \cos 2\theta),$$

and that

$$\cos 2\theta = D/R, \tag{4.10}$$

where

$$R^2 = N^2 + D^2, \tag{4.11}$$

we find

$$\alpha_1 - \alpha_2 = \tfrac{1}{2}(U_x + V_y + R), \tag{4.12}$$

which is clearly always finite. By the same process we find

$$\alpha_3 - \alpha_4 = \tfrac{1}{2}(U_x + V_y - R). \tag{4.13}$$

It can be shown that these expressions (4.12), (4.13) are proportional to the greatest and least straining rates experienced by the fluid. In these results, R must have the same sign as D, since $|\theta| \leqslant \pi/4$ and so the r.h.s. of Eq. (4.10) must be positive. For locally one-dimensional flow in the x (resp. y) direction, R will equal U_x (resp. $-V_y$) and V_y (resp. U_x) will be zero. Equations (4.12), (4.13) will give the correct one-dimensional results. That is, $\alpha_1 - \alpha_2 = U_x$ (resp. 0), and $\alpha_3 - \alpha_4 = 0$ (resp. V_y). It is interesting that

$$\alpha_1 - \alpha_2 + \alpha_3 - \alpha_4 = U_x + V_y. \tag{4.14}$$

The l.h.s. is the total strength of the acoustic waves (the minus signs appear because

of our conventions about a and θ) and the r.h.s. is the velocity divergence. Compare the result in Eq. (3.10).

The last step is to combine (4.3a), (4.3b) to give

$$\alpha_1 + \alpha_2 = P_x \cos\theta + P_y \sin\theta, \tag{4.15}$$

$$\alpha_3 + \alpha_4 = P_y \cos\theta - P_x \sin\theta, \tag{4.16}$$

and then the α's follow from (4.12), (4.13).

A remarkable identity concerning the wave strengths is the following.

$$\begin{aligned}
&\alpha_1^2 + \alpha_2^2 + \alpha_3^2 + \alpha_4^2 + \frac{1}{4}\omega^2/a^2 \\
&= \frac{1}{2}(\alpha_1 + \alpha_2)^2 + \frac{1}{2}(\alpha_1 - \alpha_2)^2 + \frac{1}{2}(\alpha_3 + \alpha_4)^2 + \frac{1}{2}(\alpha_3 - \alpha_4)^2 + \frac{\omega^2}{4a^2} \\
&= \frac{1}{2}(P_x \cos\theta + P_y \sin\theta)^2 + \frac{1}{8}(U_x + V_y + R)^2 \\
&\quad + \frac{1}{2}(P_y \cos\theta - P_x \sin\theta)^2 + \frac{1}{8}(U_x + V_y - R)^2 + \frac{\omega^2}{4a^2} \\
&= \frac{1}{2}(P_x^2 + P_y^2) + \frac{1}{4}(U_x + V_y)^2 + \frac{1}{4}R^2 + \frac{\omega^2}{4a^2} \\
&= \frac{1}{2}(P_x^2 + P_y^2) + \frac{1}{4}(U_x + V_y)^2 + \frac{1}{4}(U_x - V_y)^2 + \frac{1}{4}(U_y + V_x)^2 + \frac{1}{4}(V_x - U_y)^2 \\
&= \frac{1}{2}[P_x^2 + P_y^2 + U_x^2 + U_y^2 + V_x^2 + V_y^2].
\end{aligned} \tag{4.17}$$

Both ends of this chain are expressions representing some overall strength of the disturbance (excluding entropy effects which add another simple term).

The analysis of Model B is almost identical. The equations are altered by replacing the vorticity terms with the shear terms from (4.1) thus

$$P_x = \alpha_1 \cos\theta + \alpha_2 \cos\theta - \alpha_3 \sin\theta - \alpha_4 \sin\theta, \tag{4.18a}$$

$$P_y = \alpha_1 \sin\theta + \alpha_2 \sin\theta + \alpha_3 \cos\theta + \alpha_4 \cos\theta, \tag{4.18b}$$

$$U_x = \alpha_1 \cos^2\theta - \alpha_2 \cos^2\theta + \alpha_3 \sin^2\theta - \alpha_4 \sin^2\theta + k u_0 v_0, \tag{4.18c}$$

$$U_y = \alpha_1 \sin\theta\cos\theta - \alpha_2 \sin\theta\cos\theta - \alpha_3 \sin\theta\cos\theta + \alpha_4 \sin\theta\cos\theta - k u_0^2, \tag{4.18d}$$

$$V_x = \alpha_1 \sin\theta\cos\theta - \alpha_2 \sin\theta\cos\theta - \alpha_3 \sin\theta\cos\theta + \alpha_4 \sin\theta\cos\theta + k v_0^2, \tag{4.18e}$$

$$V_y = \alpha_1 \sin^2\theta - \alpha_2 \sin^2\theta + \alpha_3 \cos^2\theta - \alpha_4 \cos^2\theta - k u_0 v_0, \tag{4.18f}$$

$$R_x = \alpha_1 \cos\theta + \alpha_2 \cos\theta - \alpha_3 \sin\theta - \alpha_4 \sin\theta + \beta \cos\phi, \tag{4.18g}$$

$$R_y = \alpha_1 \sin\theta + \alpha_2 \sin\theta + \alpha_3 \cos\theta + \alpha_4 \cos\theta + \beta \sin\phi. \tag{4.18h}$$

The solution for β, ϕ is identical. Equations (4.18d), (4.18e) give

$$k = \frac{V_x - U_y}{u_0^2 + v_0^2}. \tag{4.19}$$

The expression for θ in this case is

$$\tan 2\theta = \frac{U_y + V_x + k(u_0^2 - v_0^2)}{U_x - V_y - 2ku_0v_0} \tag{4.20}$$

which can be rewritten, using (4.19), and setting $v/u = \tan \delta$, as

$$\tan 2\theta = \frac{U_y + V_x + (V_x - U_y)\cos 2\delta}{U_x - V_y - (V_x - U_y)\sin 2\delta} = \frac{N}{D}. \tag{4.21}$$

Note that for irrotational flow, (4.21) agrees with (4.8). Again we introduce R, such that $R^2 = N^2 + D^2$, and having the same sign as D. In terms of this new R, we still have

$$\alpha_1 - \alpha_2 = \tfrac{1}{2}(U_x + V_y + R), \tag{4.22}$$

$$\alpha_3 - \alpha_4 = \tfrac{1}{2}(U_x + V_y - R), \tag{4.23}$$

and Eqs. (4.15), (4.16) are unaffected.

For Model B there seems to be no simple analogue of Eq. (4.17). Otherwise, the difference between the two models is that Model B involves computing slightly more expensive expressions for N and D, but may be able to fit itself to a greater variety of flows. Both models have the property that if the data is locally one-dimensional in any direction then waves will be predicted which are exactly those predicted by a one-dimensional linear Riemann solver aligned in that direction (rather than with the coordinate axis). However, Model B can simultaneously recognize a shear flow in some other direction. Neither model, however, could correctly recognize both shock waves of a colliding pair, unless these happened to be perpendicular. It would appear that any model flow must be a compromise between simplicity and generality. Simple models will generally be invalid at isolated points, and reliance must then be placed on conservation. It is to this aspect that the next section is devoted.

5. Conservation Properties

To create an algorithm capable of capturing shock waves, we must ensure that it is conservative. For present purposes, the most convenient definition of a conservative algorithm is that when it operates for one time step, the conserved quantities (mass, momentum, and energy) present within the computational domain are only changed because of events occurring on the boundaries of the domain. We will first

set out a strategy which guarantees this. Then we will relate the results of previous sections to that strategy.

Suppose that the computational domain is tessellated into arbitrary polygons (see Fig. 3). Usually these would be quadrilaterals or triangles, and the formulae given below will then be very simple. However, we treat the general case to show that exceptional meshes create no difficulty, at least with regard to conservation. Consider, then, an arbitrary cell with vertices $V_1, V_2, \ldots, V_n$ and note that the area of the cell may be written

$$4A = \sum \mathbf{r}_i \times (\mathbf{r}_{i+1} - \mathbf{r}_{i-1}), \tag{5.1}$$

where $\mathbf{r}_i$ is the position vector of the ith vertex, and the counting is cyclic and anticlockwise. Equation (5.1) is proved by observing that the terms in the summation occur in equal pairs, and that every term $\mathbf{r}_i \times \mathbf{r}_{i+1}$ is twice the area of a triangle $V_i 0 V_{i+1}$, where 0 is an arbitrary origin. Rearrangement of terms in (5.1) leads to two alternative expressions

$$2A = \sum x_i (y_{i+1} - y_{i-1}) \tag{5.2}$$

$$= -\sum y_i (x_{i+1} - x_{i-1}). \tag{5.3}$$

Simple alterations of these formulae allow us to estimate the gradients within a cell of any quantity q which is defined at the vertices. Thus

$$2A \frac{\partial q}{\partial x} = \sum q_i (y_{i+1} - y_{i-1}), \tag{5.4}$$

$$2A \frac{\partial q}{\partial y} = -\sum q_i (x_{i+1} - x_{i-1}), \tag{5.5}$$

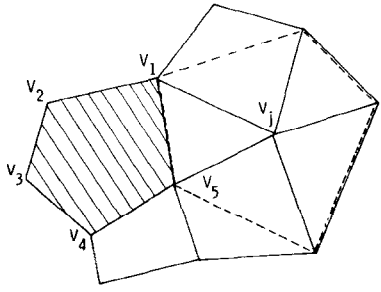

FIG. 3. Part of an irregular mesh.

and it can be seen that these estimates are exact whenever q is a linear function ($q = mx + ny$).

Now suppose that the quantities stored at the vertices are the variables defining flow of an ideal gas according to the Euler equations, written in conservation form as

$$\mathbf{w}_t + \mathbf{F}_x + \mathbf{G}_y = 0. \tag{5.6}$$

Then an estimate for $\mathbf{w}_t$, averaged over the cell, is

$$2A\mathbf{w}_t = -\sum [\mathbf{F}_i(y_{i+1} - y_{i-1}) - \mathbf{G}_i(x_{i+1} - x_{i-1})]. \tag{5.7}$$

An alternative way to obtain this formula is to integrate the passage of flux across the cell boundary, using the trapezium rule. We have followed this present derivation because the formulas (5.4), (5.5) are also useful for estimating the gradients from which, in Section 4, the local flow model was deduced.

The quantity $\mathbf{w}_t$, multiplied by a finite time step Δt reepresents the local accumulation of the conserved quantities. The solution can be advanced one time step by adding this change to the quantities stored at the vertices. The increments may be distributed equally or unequally to the vertices concerned. An equal distribution would, if applied on a regular rectangular mesh, reduce to a central-differencing scheme of the kind that can be allied with Runge-Kutta schemes [5]. An unequal distribution of increments, where the weights are obtained from the Jacobian matrices $\partial\mathbf{F}/\partial\mathbf{w}$ and $\partial\mathbf{G}/\partial\mathbf{w}$, has been used by Ni [8] to obtain an integration which is equivalent to Lax–Wendroff. The present work is intended for use with a scheme in which the increments are distributed with more regard to the "upwind" direction of each wave. By analogy with the algorithm described in Section 2 for one-dimensional flow, we propose to place the changes due to a given wave only on those vertices towards which the wave is moving. The selection of those vertices, and the weighting factors by which the effect of each wave is distributed over them will depend on the orientation of the wave relative to the cell. The details of this updating procedure are currently being studied. Meanwhile we prove that any distribution will lead to a conservative algorithm.

The total change of conserved quantities, within the computational domain, is obtained by summing (5.7) over all cells. A typical vertex V_j in the interior of the domain, contributes to this sum through all the cells which meet there. Its total contribution is, in fact

$$\Delta\mathbf{w}_j = \left[-\mathbf{F}_j \sum \Delta y + \mathbf{G}_j \sum \Delta x \right], \tag{5.8}$$

where the Δx, Δy are the adjacent chords of each cell meeting at V_j (see Fig. 3). But since the union of these chords is a closed polygon $\Delta\mathbf{w}_j = 0$. Since this argument applies equally to all interior vertices, the sum of conserved quantities changes only due to events on the boundary, and this is what we require.

Next we demonstrate how the estimated total increment (5.7) may be decom-

posed into contributions due to each wave system. It has not been found possible to do this by any direct extension of the analysis in Section 4. When the spatial changes are large, there seems to be no simple choice of mean values which allows a tidy analysis of the flux gradients. Instead, we directly analyze the temporal changes inside each cell to produce a decomposition which is conservative but not unique. Uniqueness is imposed by incorporating results from Section 4.

First, observe that the time derivative of $\mathbf{w}$ due to the passage of a plane wave is the product of the amplitude and wave speed multiplied by an eigenvector which describes the effect of that wave on the conserved variables. Such eigenvectors are easily derived as projections onto the conserved variables of the eigenvectors shown for the primitive variables in Section 3. For an acoustic wave inclined at an angle θ, the eigenvector is

$$\mathbf{r}_a = \begin{vmatrix} \rho \\ \rho u + \rho a \cos\theta \\ \rho v + \rho a \sin\theta \\ \rho h + \rho a(u\cos\theta + v\sin\theta) \end{vmatrix} \tag{5.9}$$

and for an entropy wave at any angle it is

$$\mathbf{r}_e = \begin{vmatrix} \rho \\ \rho u \\ \rho v \\ \tfrac{1}{2}\rho(u^2+v^2) \end{vmatrix}. \tag{5.10}$$

For a shear wave it is

$$\mathbf{r}_s = \begin{vmatrix} 0 \\ -\rho a \sin\theta \\ \rho a \cos\theta \\ \rho a(v\cos\theta - u\sin\theta) \end{vmatrix}. \tag{5.11}$$

However, the shear wave included in Model B has zero speed (i.e., it is a steady solution of the Euler equations) so that the term involving $\mathbf{r}_s$ makes no contribution to $\mathbf{w}_t$. In this respect Model B is somewhat simpler than Model A, because the uniform vorticity does contribute to $\mathbf{w}_t$, in a way which is derived below. Introduce the notation

$$A_1 = \alpha_1\lambda_1 = \alpha_1(u\cos\theta + v\sin\theta + a), \tag{5.12a}$$

$$A_2 = \alpha_2\lambda_2 = \alpha_2(u\cos\theta + v\sin\theta - a), \tag{5.12b}$$

$$A_3 = \alpha_3\lambda_3 = \alpha_3(-u\sin\theta + v\cos\theta + a), \tag{5.12c}$$

$$A_4 = \alpha_4\lambda_4 = \alpha_4(-u\sin\theta + v\cos\theta - a), \tag{5.12d}$$

$$A_5 = \beta\lambda_e = \beta(u\cos\phi + v\sin\phi). \tag{5.12e}$$

Our strategy is to compute the $\{A_i\}$ within each cell in such a way that the total effect of all the disturbances in that cell will produce the correct conservative value of $\mathbf{w}_t$. First, though, it must be checked that the model does contain all the effects contributing to $\mathbf{w}_t$. Therefore, we evaluate

$$\sum_{i=1}^{i=4} A_i \mathbf{r}_{ai} + A_5 \mathbf{r}_e. \tag{5.13}$$

an expression which contains the contributions to $\mathbf{w}_t$ from the plane waves used in the models, but not any contribution from the vorticity contained in Model A.

As an example, the terms contributing to ρ_t are

$$\begin{aligned}\rho[A_1 + A_2 + A_3 + A_4 + A_5] &= \rho\alpha_1(u\cos\theta + v\sin\theta a + a) \\ &\quad + \rho\alpha_2(u\cos\theta + v\sin\theta - a) + \rho\alpha_3(v\cos\theta - u\sin\theta + a) \\ &\quad + \rho\alpha_4(v\cos\theta - u\sin\theta - a) + \rho\beta(u\cos\phi + v\sin\phi) \\ &= \rho(\alpha_1 + \alpha_2)(u\cos\theta + v\sin\theta) + \rho(\alpha_1 - \alpha_2)\, a \\ &\quad + \rho(\alpha_3 + \alpha_4)(v\cos\theta - u\sin\theta) + \rho(\alpha_3 - \alpha_4)\, a \\ &\quad + \rho\beta(u\cos\phi + v\sin\phi).\end{aligned}$$

Substituting the results of Section 4 into this expression, we obtain

$$\begin{aligned}\rho[A_1 + A_2 + A_3 + A_4 + A_5] &= \rho[P_x\cos\theta + P_y\sin\theta](u\cos\theta + v\sin\theta) \\ &\quad + \rho[P_y\cos\theta - P_x\sin\theta](v\cos\theta - u\sin\theta) \\ &\quad + \tfrac{1}{2}\rho[U_x + V_y + R]\, a + \tfrac{1}{2}\rho[U_x + V_y - R]\, a \\ &\quad + \rho u[R_x - P_x] + \rho v[R_y - P_y] \\ &= \rho a[U_x + V_y] + \rho u R_x + \rho v R_y\end{aligned}$$

or, in terms of the dimensional gradients,

$$\rho[A_1 + A_2 + A_3 + A_4 + A_5] = \rho[u_x + v_y] + u\rho_x + v\rho_y = -\rho_t. \tag{5.14}$$

This calculation, which is valid for Model A or B, checks the algebra and confirms the completeness of the model. Checking the other components of $\mathbf{w}_t$ is tedious, but necessary. It reveals that Model B supplies all the terms of $\mathbf{w}_t$ from the expression (5.13), but that when this expression is used to calculate the effects of the acoustic and entropy waves in Model A, there is a shortfall in the expression for $(\rho u)_t$ amounting to $\frac{1}{2}\rho v\omega$, and a surplus in the expression for $(\rho v)_t$ of $\frac{1}{2}\rho u\omega$. These

terms represent the effects of convected vorticity. The expression for $(\rho e)_t$ turns out to be correct. Therefore, we write

$$-\rho_t = \rho(A_1 + A_2 + A_3 + A_4 + A_5), \tag{515a}$$

$$-(\rho u)_t = \rho A_1(u + a\cos\theta) + \rho A_2(u - a\cos\theta) + \rho A_3(y - a\sin\theta) + \rho A_4(u + a\sin\theta) + \rho A_5 u - \tfrac{1}{2}\rho v\omega, \tag{5.15b}$$

$$-(\rho v)_t = \rho A_1(v + a\sin\theta) + \rho A_2(v - a\sin\theta) + \rho A_3(v + a\cos\theta) + \rho A_4(v - a\cos\theta) + \rho A_5 v + \tfrac{1}{2}\rho u\omega, \tag{5.15c}$$

$$-(\rho e)_t = \rho A_1(h + au\cos\theta + av\sin\theta) + \rho A_2(h - au\cos\theta - av\sin\theta) + \rho A_3(h - au\sin\theta + av\cos\theta) + \rho A_4(h + au\sin\theta - av\cos\theta) + \tfrac{1}{2}\rho A_5(u^2 + v^2). \tag{5.15d}$$

where $\omega = 0$ for Model B.

These equations are the two-dimensional analogue of Eqs. (2.5). In each case we try to ensure that the changes of conserved variables predicted by the model are correct. Here, we assume that the *LHS* of each equation is obtained from the conservative formula (5.7) for each cell. Then we treat (5.15) as a set of conditions to be identically (not just approximately) satisfied by the $\{A_i\}$ and by θ, ϕ, ω. Since there are only four conditions for eight unknowns, the remaining information must be supplied from elsewhere. It seems natural to take the values of θ, ϕ, ω from Section 4. Conditions (5.15) are then an incomplete set of linear equations for the $\{A_i\}$, which may be partially analyzed as follows. We obtain at once

$$-(\rho u)_t + u\rho_t + \rho v\omega = \rho a\cos\theta(A_1 - A_2) - \rho a\sin\theta(A_3 - A_4), \tag{5.16a}$$

$$-(\rho v)_t + v\rho_t - \rho u\omega = \rho a\sin\theta(A_1 - A_2) + \rho a\cos\theta(A_3 - A_4), \tag{5.16b}$$

and hence $(A_1 - A_2)$, $(A_3 - A_4)$. Substituting these results into (5.15d) yields

$$\frac{\rho a^2}{\gamma - 1} A_5 = (h - u^2 - v^2)\rho_t + u(\rho u)_t + v(\rho v)_t - (\rho e)_t. \tag{5.17}$$

If the changes are so small that $(\cdot)_t$ may be treated as a derivative, rather than as a numerical estimate of a derivative, these equations simplify considerably, offering more insight into the models.

$$(A_2 - A_1) = u_t\cos\theta + v_t\sin\theta - \tfrac{1}{2}(v\cos\theta - u\sin\theta)\omega, \tag{5.18}$$

$$(A_4 - A_3) = v_t\cos\theta - u_t\sin\theta + \tfrac{1}{2}(u\cos\theta + v\sin\theta)\omega, \tag{5.19}$$

$$A_5 = (a^2\rho_t - p_t)/\rho a^2, \tag{5.20}$$

$$A_1 + A_2 + A_3 + A_4 = p_t. \tag{5.21}$$

Nonconservative schemes could use these simpler conditions; a fully conservative scheme would have to satisfy (5.15).

One more condition is needed on the $\{A_i\}$. In view of the symmetry of the results so far, we would like an expression for $A_1 + A_2 - A_3 - A_4$ (which need not derive from the conservation form). By changing some signs in the analysis leading to (5.14) we find

$$A_1 + A_2 - A_3 - A_4 = P_x(u \cos 2\theta + v \sin 2\theta) + P_y(u \sin 2\theta - v \cos 2\theta) + aR. \tag{5.22}$$

It may be shown that the r.h.s. does not, in general, vanish when the data are taken from a steady flow. One might suppose that it should, since then the $\{A_i\}$ would all be zero, and either the strength or the speed of every wave would be zero. Instead of this, the models represent steady flow by a state of equilibrium between finite waves, such that $A_1 = A_2 = -A_3 = -A_4$, and $A_5 = 0$.

We have now generated a conservative model of the flow, in which the effects of the various components are given by (5.15). The parameters of this decomposition ($\{A_i\}, \theta, \phi, \omega$) are found from (4.4), (4.5), (4.8), or (4.21), (5.16), (5.17), and (5.22). Any consistent choice of local average values for ρ, u, v, a, h in these equations will be valid, and will not affect the conservation property. It may be asked, though, whether there are particular average values, similar to those which appear in the one-dimensional theory [9, 12], bestowing special "shock-recognition" properties. However, this question raises unsolved problems about the sort of "captured shock structure" that is possible in two-dimensional flow, and will not be discussed here.

6. Extension to Three Dimensions

No detailed formulae have been worked out for the three-dimensional case. However, merely counting the degrees of freedom makes it plausible that analogous models could be constructed. Data for the three-dimensional unsteady Euler equations would consist of five variables, so there would be fifteen gradients to be accounted for by the model. If the acoustic disturbances are again to be represented by a set of orthogonal plane waves (like an expanding cube) there will be six wave amplitudes and three angles involved (two angles to orient one wave, one angle to orient its neighbors). An entropy wave with one amplitude and two angles will bring the number of parameters up to twelve. The remaining three are available to represent rotational effects. The analogue of Model A would contain three independent vorticity components. The analogue of Model B could contain a shear flow

$$\mathbf{q} = \mathbf{q}_0[1 + k_1(v_0 x - u_0 y) + k_2(w_0 y - v_0 z) + k_3(u_0 z - w_0 x)] \tag{6.1}$$

which is, like (5.1), a steady solution to the Euler equations. However, the three shear components which it contains are not all independent, since all take place in a

parallel flow, and one of the k_i can be dropped with no loss of generality. To complete the set of fifteen parameters one might add the flow

$$\begin{aligned} u &= u_0 = \omega(w_0 y - v_0 z), \\ v &= v_0 + \omega(u_0 z - w_0 x), \\ w &= w_0 + \omega(v_0 x - u_0 y). \end{aligned} \tag{6.2}$$

This is also a steady solution of the Euler equations and represents a swirling flow in which the vorticity is parallel to the streamline (u_0, v_0, w_0). Again there is a computational advantage to Model B in that some of its components are steady flows whose contribution to the time-marching process are identically zero. In fact, an analogue of Model B can be worked out for any number of space dimensions d, and the description of arbitrary data is reduced to the description of $(2d+1)$ non-linear scalar advection problems.

There are, however, geometrical difficulties which appear in three dimensions, if the partition of space is made into volumes whose facets have more than three sides. Most finite-volume schemes employ computational cells which are hexahedral, with quadrilateral faces specified by four vertices not normally lying in one plane. The boundary surfaces of the cells must be unambiguously defined so that the cells fill the computational space without overlaps or voids. This can be done by folding each surface into two triangles [6], or by choosing a particular doubly ruled surface to cover each face [3]. Once this has been done, any consistent formula for the volume can also be used to estimate the flux divergence, as in (5.7), but the consistent formulae are disconcertingly lengthy [6, 3]. The effect of simpler formulae on the computational accuracy awaits investigation.

7. Advection Schemes

The eventual goal of this work is to create an algorithm for multidimensional gas dynamics which will enjoy the same degree of success already obtained by upwind schemes in one dimension. In this paper we have addressed (at most) half the problem, showing how arbitrary disturbances in the data can be replaced by locally equivalent sets of plane waves and/or vorticity. To march forward in time, we need to apply to each wave some numerical advection scheme. We may hope that such schemes can be based on schemes for scalar problems, as has happened in the one-dimensional case. Also, we may anticipate that such schemes will show many of the typical features of successful one-dimensional schemes, such as asymmetric support and non-linear limiters [15]. However, the theory even of scalar advection algorithms in many dimensions is only in its infancy. Roe and Baines [11] present a criterion designed to avoid overshoots and describe a scheme which meets it. Smolarkiewicz [14] describes another distinctive, but related, approach. The next

(rather large) step in the investigation reported here will be to experiment with these and other algorithms in the present context.

8. Conclusions

We have pointed out that the extension of upwind differencing schemes to more than one space dimension cannot be accomplished by operator splitting methods without losing the desirable property of recognizing data due to a simple wave. To construct "genuinely two-dimensional" schemes we propose model flows, composed of elementary solutions to the two-dimensional equations. These model flows are such that they can be matched to arbitrary data which varies linearly in some small region. The acoustic part of the flow is modelled by four orthogonal plane waves whose orientation is matched to the gradients in the data. Variation of entropy is represented by a single plane wave, and rotational effects either by uniform vorticity or by a parallel shearing motion. We show that the parameters of the model can be evaluated in such a way that a time-marching algorithm can be made exactly conservative.

References

1. S. R. Chakravarthy and S. Osher, *in* "Large-Scale Computations in Fluid Mechanics," Lectures in Applied Mathematics, Vol. 22, AMS 1985.
2. P. Colella, Multidimensional upwind methods for hyperbolic conservation law, Lawrence Berkeley Laboratory, Berkeley, Calif., preprint, LBL-17023, 1984.
3. D. E. Davies and Deborah Salmond, "Calculation of the volume of a general hexahedron for flow predictions," *AIAA J.* **23** (6) (1985), 954.
4. S. F. Davis, *J. Comput. Phys.* (1984), 65.
5. A. Jameson, W. Schmidt, and E. Turkel, "Numerical solutions of the Euler equations by finite-volume methods using Runge-Kutta time-stepping schemes," AIAA Paper 81-1259, 1981.
6. W. Kordulla and M. Vinokur, *AIAA J.* **21** (1983), 917.
7. C. C. Lytton (Formerly C. C. L. Sells), "Solution of the Euler Equations for Transonic Flow Past a Lifting Airfoil—The Bernoulli Formulation," Royal Aircraft Establishment, TR 84080, 1984.
8. R-H. Ni, *AIAA J.* **20** (11) (1982), 1565.
9. P. L. Roe, *J. Comput. Phys.* (1981), 357.
10. P. L. Roe, *in* "Proceedings, INRIA Workshop on Numerical Methods for the Euler Equations," SIAM, 1985, to appear.
11. P. L. Roe and M. J. Baines, *in* "Proceedings 5th GAMM Conference on Numerical Methods in Fluid Mechanics" (M. Pandolfi and R. Piva, Eds), Vieweg, Brunswick, 1984.
12. P. L. Roe and J. Pike, *in* "Computing Methods in Applied Sciences and Engineering VI" (R. Glowinski and J-L. Lions, Eds.), pp. 499–518, North-Holland, Amsterdam, 1984.
13. C. C. L. Sells, "Solution of the Euler Equations for Transonic Flow Past a Lifting Airfoil," Royal Aircraft Establishment, TR 80065, 1980.
14. P. K. Smolarkiewicz, *J. Comput. Phys.* **54** (1984), 325.
15. P. K. Sweby, *SINUM* **25** (5) (1984), 995.
16. P. Woodward and P. Colella, *J. Comput. Phys.* (1984), 115.